Ab initio evidence for the formation of impurity $d_{3z^2-r^2}$ holes in doped $La_{2-x}Sr_xCuO_4$

Jason K. Perry,[1,2] Jamil Tahir-Kheli,[1,2] and William A. Goddard III[2]
[1]*First Principles Research, Inc.,* 6327-C SW Capitol Highway, PMB 250, Portland, Oregon 97201*
[2]*Materials and Molecular Simulation Center, Beckman Institute, California Institute of Technology, Pasadena, California 91125*
(Received 14 November 2001; published 8 March 2002)

Using the spin unrestricted Becke-3-Lee-Yang-Parr density functional, we computed the electronic structure of explicitly doped $La_{2-x}Sr_xCuO_4$ ($x=0.125$, 0.25, and 0.5). At each doping level, an impurity hole band is formed within the undoped insulating gap. This band is well localized to CuO_6 octahedra adjacent to the Sr impurities. The nature of the impurity hole is A_{1g} in symmetry, formed primarily from the z^2 orbital on the Cu and p_z orbitals on the apical O's. There is a strong triplet coupling of this hole with the intrinsic B_{1g} Cu x^2-y^2/O1 p_σ hole on the same site. Optimization of the c coordinate of the apical O's in the doped CuO_6 octahedron leads to an asymmetric anti-Jahn-Teller distortion of the O2 atoms toward the central Cu. In particular, the O2 atom between the Cu and Sr is displaced 0.26 Å while the O2 atom between the Cu and La is displaced 0.10 Å. Contrary to expectations, investigation of a 0.1 Å enhanced Jahn-Teller distortion of this octahedron does not force formation of an x^2-y^2 hole, but instead leads to migration of the z^2 hole to the four other CuO_6 octahedra surrounding the Sr impurity. This latter observation offers a simple explanation for the bifurcation of the Sr-O2 distance revealed in x-ray absorption fine structure data.

DOI: 10.1103/PhysRevB.65.144501 PACS number(s): 74.25.Jb, 71.15.Mb

INTRODUCTION

The electronic structure of the cuprates obtained by the local spin density approximation (LSDA)[1] holds an unusual position in the field of superconductivity research. It is considered a failure because it is unable to produce the undoped insulating ground state and does not explain the normal state properties of the doped materials. Yet despite these significant shortcomings, LSDA has in no small way contributed to the consensus view that the only orbitals relevant to cuprate superconductivity are the Cu x^2-y^2 and O1 planar p_σ orbitals. Other orbitals, in particular the Cu z^2 and apical O2 p_z orbitals, were determined to be well below the Fermi level, and therefore not relevant. This assumption colors the interpretation of virtually every experiment and imposes clear constraints on theories of superconductivity in these materials.

The endurance of the LSDA results regarding the relevant orbitals near the Fermi level is odd given that more advanced density functionals have hinted at a more complicated picture. In particular, the failure of LSDA regarding the undoped state was addressed in the early 1990's by several groups. Svane,[2] and later Temmerman *et al.*,[3] considered a self-interaction correction (SIC) LSDA, in which the self-Coulomb term that a localized electron improperly sees with itself in a conventional LSDA is removed. Anisimov *et al.*[4] took a somewhat similar approach with the LSDA+U method, as did Czyzyk and Sawatzky.[5] All achieved some success in producing an insulating gap of the right magnitude in La_2CuO_4, correcting the most glaring flaw in the LSDA.

Perhaps the most important and most overlooked point raised in these studies is the consistent observation of a marked increase in Cu z^2 and O2 p_z character at the top of the valence band. The basic nature of the undoped hole state (a hybrid Cu x^2-y^2 and O1 p_σ orbital) is unchanged with respect to the LSDA. But these calculations all suggest the formation of at least some z^2 holes upon doping, in direct contradiction to the conventional LSDA model.

Further evidence for z^2 character at the Fermi level appeared when Anisimov *et al.*[4] took their calculations a step farther by considering the effect of implicit and explicit Sr doping in $La_{1.75}Sr_{0.25}CuO_4$. In both cases the LSDA+U approach found the doped hole to be a localized Cu x^2-y^2/O1 p_σ hybrid in the undistorted crystal, in support of the LSDA picture. However, when they allowed a distortion of the apical O2 atoms about the doped hole, they found a local minimum where the hole changed to a localized Cu z^2/O2 p_z hybrid. This anti-Jahn-Teller state was found to be only 54 meV above the global minimum. The distortion was constrained to be symmetric (both apical O2 atoms moved 0.26 Å toward the central Cu) and only performed for the implicitly doped case. An asymmetric distortion was not investigated nor was a distortion in the explicitly doped case. Both of these situations should be more favorable for this anti-Jahn-Teller state.

Recently, an x-ray absorption fine structure (XAFS) study by Haskel and co-workers[6] concluded that a majority of Sr impurities in $La_{2-x}Sr_xCuO_4$ induced such an anti-Jahn-Teller state, with the Sr-O2 distance increasing by 0.2 Å. A minority of Sr impurites lead to an enhanced Jahn-Teller distortion, with the Sr-O2 distance decreasing by 0.1 Å. As the results of Anisimov *et al.*[4] are somewhat ambiguous, this intriguing experimental finding invites a reconsideration of the *ab initio* description of the doped state.

In a series of papers,[7] we have argued against the LSDA single band picture and presented a model for the cuprate band structure involving the stabilization of the Cu x^2-y^2/O1 p_σ band (herein referred to as x^2-y^2) with respect to the Cu z^2/O2 p_z band (herein referred to as z^2). This model leads to a Fermi level crossing of the narrow z^2 band and the broad x^2-y^2 band along the $(0,0)$–(π,π) direction of the three-dimensional (3D) Brillouin zone and is consistent with sev-

eral important and otherwise anomalous features of the NMR, ARPES, Hall effect, and Josephson tunneling.

Most recently, we took advantage of some modern developments in density functional theory (DFT) and looked at the electronic structure of undoped La_2CuO_4 using the unrestricted spin form of the Becke-3-Lee-Yang-Parr functional (U-B3LYP).[8] This hybrid functional, developed since the first LSDA calculations were performed on the cuprates, incorporates both gradient corrections and 20% Hartree-Fock exchange.[9] It has attained a high level of popularity for its accurate treatment of molecular systems, and indeed, this ''off-the-shelf'' functional successfully produced a 2.0 eV insulating band gap in La_2CuO_4, in excellent agreement with experiment. As with the SIC-LSDA and LSDA+U calculations,[2–5] a significant increase in Cu z^2/O2 p_z character at the top of the valence band was noted.

In this work, we consider how the U-B3LYP functional describes the doped material $La_{2-x}Sr_xCuO_4$ ($x=0.125$, 0.25, and 0.5), using supercells of size $8\times$, $4\times$, and $2\times$, respectively. The combination of this new functional and explicit doping produces a clear *ab initio* picture of the cuprates fundamentally different from LSDA. At each doping level, holes are inhomogeneously created on one CuO_6 octahedron adjacent to each Sr impurity. Localization of the doped holes is consistent with nuclear quadrupole resonance (NQR) data which clearly resolves two inequivalent Cu sites in doped $La_{2-x}Sr_xCuO_4$ and $La_2CuO_{4+\delta}$.[10] Our calculations reveal the holes are dominated by Cu z^2 and O2 p_z character. These holes are triplet coupled to the intrinsic holes on the doped site, leading to the formation of a spin-polarized impurity band within the insulating gap. Independently optimizing the *c* axis coordinates of the O2 atoms, we find an anti-Jahn-Teller distortion about the doped site similar to the local minimum found by Anisimov *et al.*[4] Furthermore, we find an enhanced Jahn-Teller distortion of these same apical O2 atoms leads to migration of the z^2 hole to different CuO_6 octahedra around the impurity. This latter observation suggests a simple explanation for the bifurcation of the Sr-O2 distance seen in the XAFS data of Haskel and co-workers.[6] While the important issue of disorder will be addressed in a separate article, the U-B3LYP picture is unequivocal. The doped hole in $La_{2-x}Sr_xCuO_4$ is localized near the impurity and is z^2 in character.

As we have already documented the superiority of this functional in describing the undoped cuprate, this new picture must be regarded as a serious challenge to LSDA. The clear implication from this work is that models of superconductivity should not be constrained to consider only the Cu x^2-y^2 and O1 p_σ orbitals. They must consider the Cu z^2 and O2 p_z orbitals as well.

RESULTS AND DISCUSSION

Calculations were performed using a modified version of CRYSTAL98.[11] To handle the large number of two electron integrals generated in the $x=0.125$ calculations (>70 gigabytes), we altered the way CRYSTAL98 manages these files. We also incorporated Johnson's modification of the Broyden procedure to improve general convergence.[12] For O, the standard 8-51G Gaussian type basis set was used.[13] For Cu, Sr, and La, the Hay and Wadt effective core potentials (ECP's) were used.[14] The valence electrons and outer core ($3s$ and $3p$ for Cu, $4s$ and $4p$ for Sr, and $5s$ and $5p$ for La) were treated explicitly with these ECP's. The basis sets used were modified from the original basis sets of Hay and Wadt, since some functions are too diffuse for calculations on crystals. For Cu, the two diffuse *s* exponents were replaced by a single exponent optimized to 0.30 in our previous publication on undoped La_2CuO_4.[8] The two Cu diffuse *p* exponents were replaced by a single exponent optimized to 0.20. The basis set was contracted to $(3s3p2d)$ based on atomic Cu(II) calculations. For La, the two diffuse *s*, two diffuse *p*, and the diffuse *d* exponents were removed. The basis set was contracted to $(2s2p1d)$ based on atomic La(III) and La(II) calculations. To this the core *s* function of the standard Sr 31G basis set[13] was added, and the combined $(3s2p1d)$ basis set was used for both La and Sr sites. The overall basis set is smaller than that used previously,[8] but tests with larger basis sets did not lead to any qualitative change in the results for either the undoped or $x=0.50$ doped materials.

TABLE I. Direct lattice vectors for the $2\times$, $8\times$, $4\times$, and $2\times$ supercells of $La_{2-x}Sr_xCuO_4$, where $x=0.0$, 0.125, 0.25, and 0.5, respectively (in Å).

	−1.906	1.906	6.609
$x=0.0$	1.906	−1.906	6.609
	3.812	3.812	0.000
	−7.624	−7.624	0.000
$x=0.125$	7.624	−7.624	0.000
	1.906	5.718	6.609
	−7.624	0.000	0.000
$x=0.25$	0.000	7.624	0.000
	1.906	1.906	−6.609
	−1.906	1.906	6.609
$x=0.50$	1.906	−1.906	6.609
	3.812	3.812	0.000

The tetragonal La_2CuO_4 crystal structure ($I4/mmm$) was taken from Hazen.[15] The lattice parameters of the conventional cell are $a=b=3.812$ Å and $c=13.219$ Å. All calculations, including undoped, were run in appropriate supercells ($2\times$ for $x=0.0$ and $x=0.5$, $4\times$ for $x=0.25$, and $8\times$ for $x=0.125$). The direct lattice vectors for these supercells are given in Table I. The positions of the irreducible Cu, O1, and La/Sr atoms in the conventional cell were taken from Hazen: Cu = (0.0000, 0.0000, 0.0000), O1 = (0.5000, 0.0000, 0.0000), and La/Sr = (0.0000, 0.0000, 0.3614). However, the position of the O2 atom was optimized for each doping level. For the undoped material, the optimal position was calculated to be O2 = (0.0000, 0.0000, 0.1812). This gives a Cu-O2 distance of 2.40 Å, in good agreement with crystallography data of 2.43 Å. Optimization of other coordinates was considered on a limited basis, as noted below.

The undoped band structure, calculated in a $2\times$ supercell

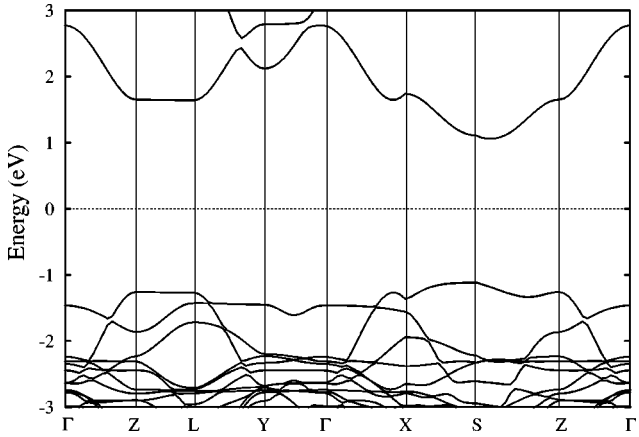

FIG. 1. Band dispersion plotted along symmetry lines of the orthorhombic Brillouin zone (see Ref. 8) from the U-B3LYP calculation of La_2CuO_4. Results are in good agreement with the SIC-LSD and LSDA+U computations of Refs. 2–5.

$(Bmab)$, is shown in Fig. 1. Unlike the LSDA, ↑ and ↓ spins localize on adjacent Cu's, producing the expected 2.1 eV band gap. The results are in good agreement with SIC-LSDA (Refs. 2,3) and LSDA+U (Refs. 4,5) band structures as well as our previous U-B3LYP calculations[8] which employed a larger basis set. As described in our previous work, analysis of the density of states (DOS) indicates the undoped hole is composed almost entirely from the Cu x^2-y^2 and O1 p_σ orbitals, consistent with the standard model. However, there is a notable increase in the Cu z^2 and O2 p_z DOS at the top of the valence band as compared to the LSDA. The top 0.15 electrons/unit cell of the valence band are 52% Cu z^2/O2 p_z. This value is slightly larger than what we computed previously (40%), perhaps due to the change in basis set or due to the change in the O2 geometry, but the observation of significant A_{1g} orbital character at the top of the valence band is in qualitative agreement with other DFT methods that achieved an insulating ground state.[2–5] As we have discussed in several publications,[7,8] this increase in z^2 character at the Fermi level is the result of a stabilization of the x^2-y^2 band due to a proper accounting of on-site Coulomb repulsion. In the LSDA, it is widely agreed that this Coulomb repulsion is overestimated.[2–5] A consequence of this is that the x^2-y^2 band is raised in energy relative to the fully occupied bands. As articulated in our previous work, this observation alone casts some doubt on the validity of the LSDA single band picture.

A common approach to understanding the doped state involves starting with the band structure for the undoped material and removing the appropriate number of electrons. Adopting such a rigid band model with the undoped LSDA band structure would suggest the system is homogeneously doped by removing additional electrons from the x^2-y^2 band.[1] A rigid band model from the undoped U-B3LYP band structure would also suggest the system is homogeneously doped by forming a mixture of x^2-y^2 and z^2 holes. However, the rigid band approach is questionable given NQR (Ref. 10) and XAFS (Ref. 6) data which suggest the doped cuprates are both electronically and structurally inhomogeneous. To examine this issue, we have calculated the U-B3LYP band structures for explicitly doped $La_{2-x}Sr_xCuO_4$.

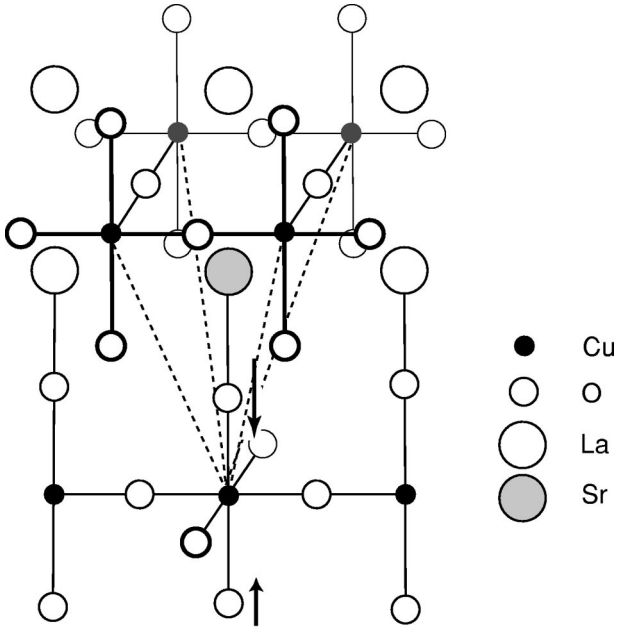

FIG. 2. Schematic of the crystal structure around a Sr impurity in $La_{2-x}Sr_xCuO_4$. The Cu atom is at the apex of a square pyramid about the impurity, and Cu′ and Cu″ form the base. The Cu′ and Cu″ atoms are distiguished by spin.

Doping is achieved by making a substitution of a Sr atom for a single La atom in the appropriate supercell, breaking the degeneracy of the Cu sites. For each doping level ($x=0.125$, 0.25, and 0.5), the same behavior was observed: doped holes are formed inhomogeneously in the vicinity of the impurity. In Fig. 2, we show schematically the crystal structure about the Sr impurity. There are five Cu atoms surrounding the Sr in a square pyramidal geometry. The atom labeled Cu in Fig. 2 is at the apex, and the atoms labeled Cu′

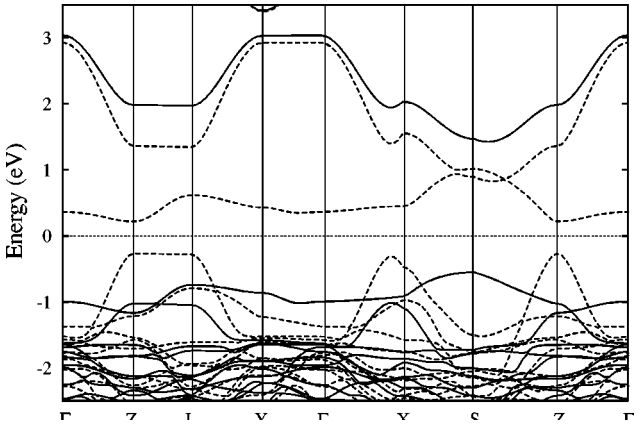

FIG. 3. Band dispersion plotted along symmetry lines of the orthorhombic Brillouin zone from the U-B3LYP calculation of $La_{1.5}Sr_{0.5}CuO_4$. Solid line: ↑ spin. Dashed line: ↓ spin. The splitting of the doped ↓ spin z^2 band (the dashed lined just above the Fermi level) and the undoped ↑ spin z^2 band (the solid line just below the Fermi level) is clearly visible.

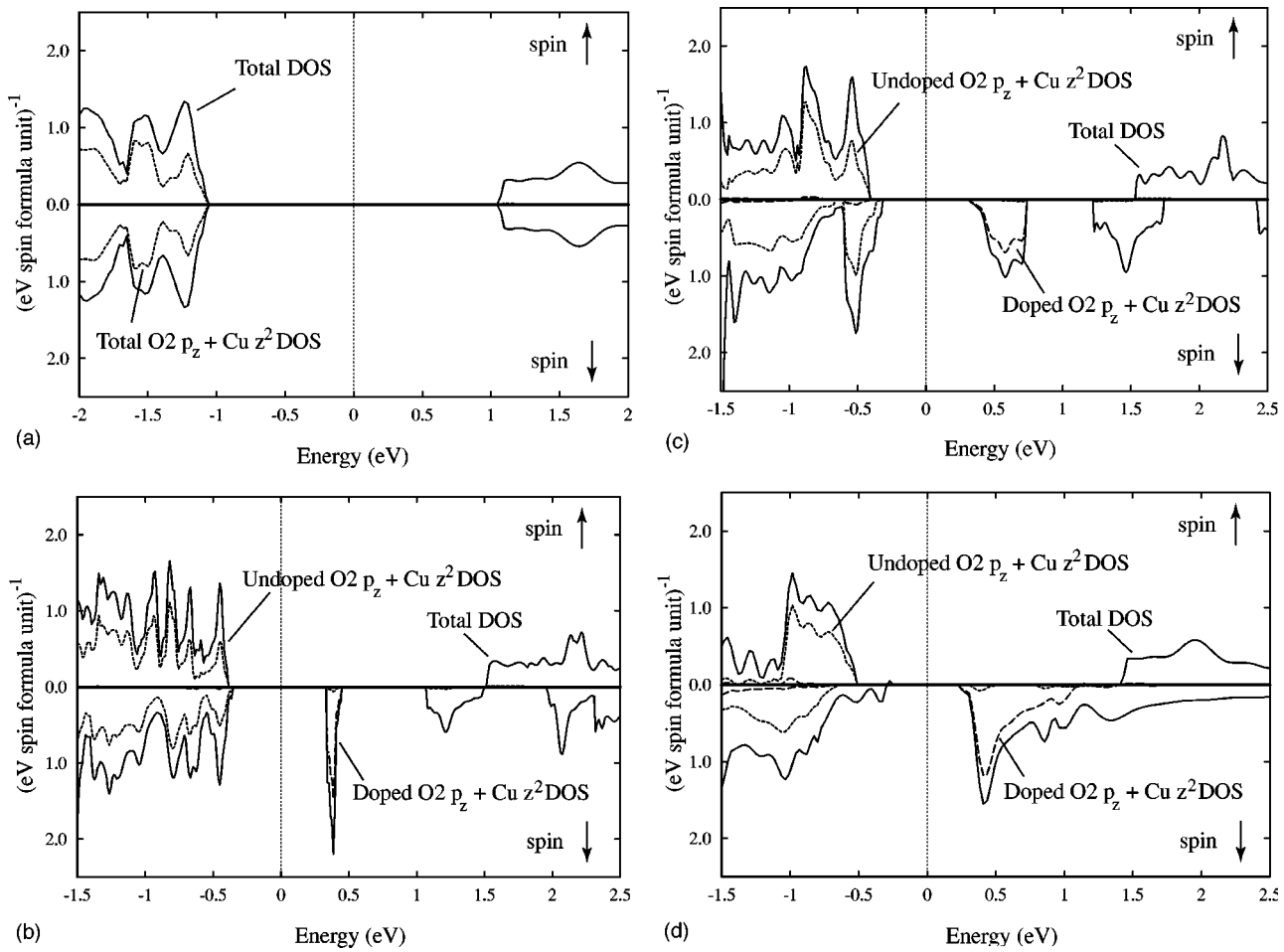

FIG. 4. Density of states from the U-B3LYP calculations of $La_{2-x}Sr_xCuO_4$ (a) $x=0.0$, (b) $x=0.125$, (c) $x=0.25$, (d) $x=0.5$. Solid line: total DOS. Dashed line: Cu z^2 + O2 p_z DOS at doped sites. Dotted line: Cu z^2 + O2 p_z DOS at undoped sites.

and Cu″ form the base. The latter pairs of Cu atoms are distinguished by spin. Of these five Cu atoms, it is the apex Cu that is preferentially doped. Thus we define the doped unit as the CuO_6 octahedron associated with this apex Cu. The holes formed in the doped unit are dominantly A_{1g} Cu z^2/O2 p_z in character and triplet coupled to the B_{1g} Cu x^2-y^2/O1 p_σ intrinsic holes on the same site. Since there is only one doped site per supercell, symmetry dictates that all of the doped holes will be of the same spin. It is important to realize that this would not be the case in the real system, where the distribution of doped sites is random. Indeed, we expect a random distribution of Sr sites to have a profound effect on the band structure, restoring approximate single unit cell symmetry in particular. But there is no reasonable expectation that this would significantly alter either the z^2 orbital character of the holes or the triplet coupling of these holes to the x^2-y^2 holes. Understanding these caveats, in these highly ordered doped materials, the degeneracy of the ↑ and ↓ spin bands is lifted. A new ↓ spin z^2 hole band appears in the undoped insulating gap, having a width which is dependent on the doping level. The band structure for $x=0.5$ is shown in Fig. 3. The minority spin (↓ spin) doped z^2 band lies entirely above the Fermi level.

More detailed information on the nature of the doped holes can be obtained from the DOS given in Fig. 4 and Table II. The nature of the holes on the undoped sites is relatively unchanged upon doping. The Cu x^2-y^2 hole character ranges from 0.552 at $x=0.0$ to 0.602 at $x=0.50$. A similar small increase in hole character upon doping is also observed on the neighboring O1 atoms. In contrast, the nature of the holes on the doped sites is markedly different.

TABLE II. Populations per atom for doped and undoped sites. Doped sites are defined as the CuO_6 unit in line with the Sr impurity along the *c* axis (see Fig. 2). Undoped sites refer to all other atoms.

doped	Cu x^2-y^2	Cu z^2	O2 p_z	O2' p_z	O1
$x=0.125$	0.410	0.341	0.238	0.086	0.227
$x=0.25$	0.418	0.367	0.227	0.108	0.245
$x=0.5$	0.425	0.375	0.224	0.140	0.267
undoped	Cu x^2-y^2	Cu z^2	O2	O1	
$x=0.0$	0.552	0.003	0.005	0.180	
$x=0.125$	0.567	0.005	0.008	0.195	
$x=0.25$	0.581	0.028	0.010	0.210	
$x=0.5$	0.602	0.015	0.019		

There is significant Cu z^2 hole character (ranging from 0.341 at $x=0.125$ to 0.375 at $x=0.5$), as well as O2 p_z hole character (ranging from 0.238 to 0.224 on the O2 between the Cu and Sr and 0.086 to 0.140 on the O2 between the Cu and La). Inspection of Fig. 4 reveals that this Cu z^2/O2 p_z character can be isolated to the band which appears in the insulating gap upon doping. This band increases in width upon doping (from ≈ 0.1 eV at $x=0.125$ to ≈ 0.8 eV at $x=0.5$), reflecting an increase in coupling between doped sites as their concentration increases. The split in the x^2-y^2 $\downarrow$ spin hole band should also be noted, particularly in the $x=0.125$ and $x=0.25$ DOS figures. The lower energy component is dominated by the doped site x^2-y^2 orbital, while the higher energy component is dominated by the undoped site x^2-y^2 orbital. Interestingly, the Cu x^2-y^2 hole character *decreases* on the doped sites (from 0.552 at $x=0.0$ to 0.410 at $x=0.125$ and 0.425 at $x=0.5$). This decrease in Cu x^2-y^2 hole character is compensated by an increase in p_σ hole character on the neighboring O1 atoms. This redistribution of charge in the x^2-y^2 band effectively minimizes the formation of unfavorable Cu(III) states when holes are formed in the z^2 band.

As stated earlier, the position of the apical O2 atoms along the *c*-axis was optimized for each doping level. For $x=0.5$ there are four unique O2 atoms. For $x=0.25$ there are six, and for $x=0.125$ there are eight. The positions of all four O2 atoms in the $x=0.50$ state were optimized independently. The O2 atom between the Sr and Cu in the doped unit moved away from the Sr atom and toward the Cu by 0.24 Å. The O2 atom between the La and Cu of this doped unit moved toward the Cu by 0.10 Å. The O2 atoms of the undoped CuO_6 octahedra both moved a negligible amount in the direction away from the Sr impurities (0.03 and 0.02 Å). Investigation of Sr and La *c*-axis displacement indicated that the Sr moved toward the doped CuO_6 octahedron by 0.02 Å while the La atoms were unchanged. Thus, the Sr-O2 distance increased overall by 0.22 Å relative to the La-O2 distance. Investigation of O1 atom displacements in the *ab* plane showed no change in their positions. The well-known CuO_6 tilt was not investigated. Given the small displacements of the undoped O2 atoms and the Sr, we chose to only optimize the *c*-axis position of the two O2 atoms in the doped unit for $x=0.125$ and $x=0.25$. The results are virtually identical to the displacements seen at $x=0.50$. At both $x=0.125$ and $x=0.25$, the O2 atom between the Sr and Cu moved 0.26 Å toward the Cu, while the O2 atom between the La and Cu moved 0.11 Å toward the Cu. While Anisimov *et al.*[4] only considered a symmetric distortion of the apical O's about the doped site, the 0.26 Å displacement that they reported is in agreement with our data.

The finding of a localized hole in these calculations is consistent with NQR data which reveals two distinct types of Cu's in the doped superconductor.[10] The anomalous "*B*" sites have been shown to increase with doping, and their appearance is independent of the dopant (Sr or excess O). The NQR data provide strong support for localized hole formation, something the standard LSDA band structure fails to predict.[1] Analysis by Hammel *et al.*[10] suggests the hole is localized in a CuO_6 octahedron adjacent to the impurity. Indeed, a large anti-Jahn-Teller distortion at the apex Cu site around the impurity is found in the XAFS data of Haskel and co-workers.[6] In some samples, they found an anti-Jahn-Teller distortion of 0.15 Å for the O2 atom between the Cu and Sr. In other samples (differing in preparation procedure), they found a bifurcation of the O2 position, where an anti-Jahn-Teller distortion of ≈ 0.2 Å was observed at a majority of

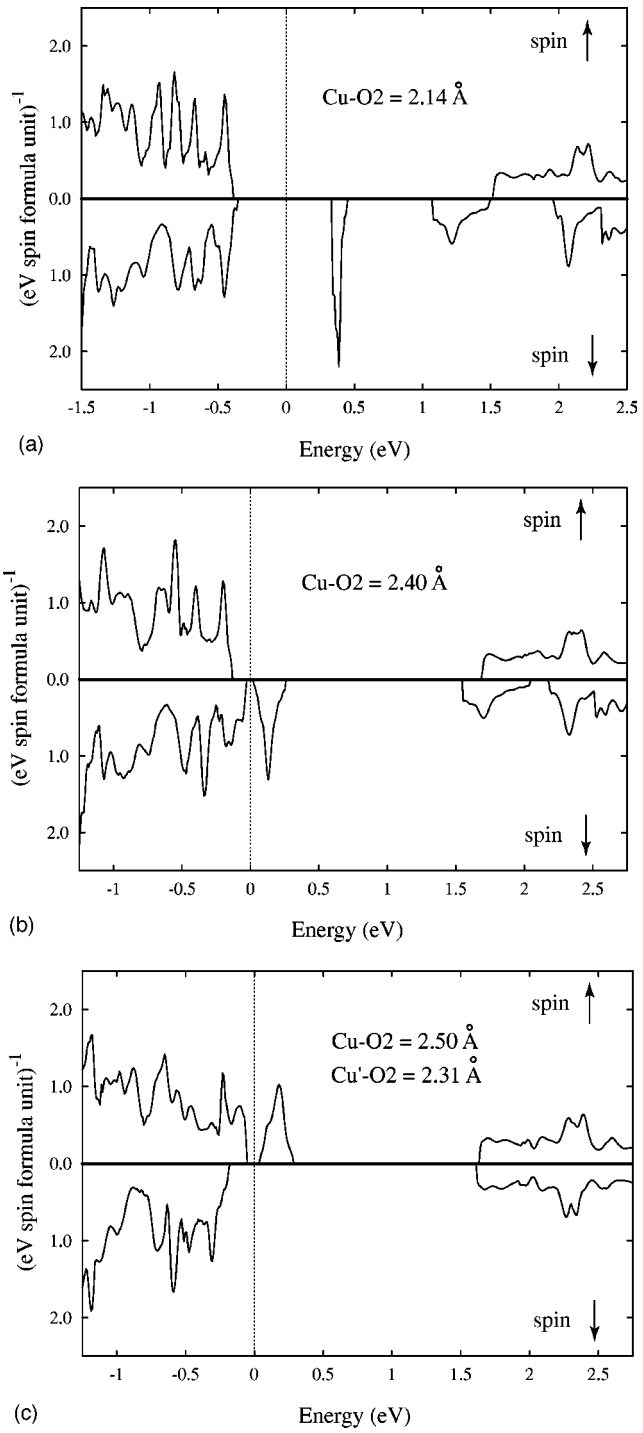

FIG. 5. Density of states from calculations on $La_{1.875}Sr_{0.125}CuO_4$ for (a) the anti-Jahn-Teller distorted optimal structure, (b) the unoptimized (undoped) structure, and (c) the enhanced Jahn-Teller structure.

sites and an enhanced Jahn-Teller distortion of ≈ 0.1 Å was observed at a minority of sites. This structural bifurcation could not be observed in these calculations due to the symmetry of the supercells employed. However, our calculations are in quantitative agreement with the anti-Jahn-Teller distortion at the doped site.

To also gain insight into the enhanced-Jahn-Teller state, we calculated the band structure for $x=0.125$ moving the O2 atom between the Sr and Cu 0.1 Å toward the Sr. Given this distortion, we optimized the *c*-axis position of the other four O2 atoms about the Sr impurity. All other atoms were left in their undoped positions. A comparison of the DOS for the anti-Jahn-Teller distorted optimal structure, the unoptimized structure, and this enhanced Jahn-Teller structure for $x=0.125$ is given in Fig. 5. The main change observed in the DOS with the movement of this O2 atom is the shift in the z^2 hole band. For the anti-Jahn-Teller distorted optimal structure, this z^2 band is in the middle of the undoped insulating gap. For the undistorted structure, this band is near the bottom of the gap. But for the enhanced Jahn-Teller structure, the z^2 band is stabilized such that holes are formed in another band. A detailed analysis of the DOS reveals that the z^2 holes migrate to either the two Cu′ octahedra adjacent to the impurity (having a spin opposite to the apex Cu) or to the two Cu″ octahedra adjacent to the impurity (having a spin parallel to the apex Cu). At certain geometries it was possible to form holes on all five Cu's surrounding the impurity, but optimization of the O2 atoms led to localization. Here we have shown the particular localization where z^2 holes form at the Cu′ sites. The apical O's associated with the Cu′ atoms undergo an anti-Jahn-Teller distortion of 0.09 Å while the apical O's associated with the two Cu″ atoms see no such distortion. Given the very small gap between the z^2 electrons and the z^2 holes on the doped sites, we expect the z^2 hole to further localize to just one of the Cu′ octahedra. Symmetry constraints prevent this in these calculations.

With respect to the anti-Jahn-Teller optimized structure, this enhanced-Jahn-Teller state is 0.57 eV higher in energy (71 meV per $La_{1.875}Sr_{0.125}CuO_4$ unit cell). While the ground state of this highly ordered doped structure is well defined, these calculation indicate the doped z^2 hole could form at any of the five Cu atoms surrounding the impurity. We suggest the observed bifurcation in the Sr-O2 distance is due to migration of the z^2 holes to alternative sites when the locations of the impurities is random. In order to produce a more uniform distribution of doped holes given random impurities, in some cases it may be favorable to form holes at either the Cu′ or Cu″ sites leading to an enhanced Jahn-Teller distortion of the apex O2 atom. In the majority of cases, holes should be formed at the apex Cu as described in this work, leading to an anti-Jahn-Teller distortion of the apex O2 atom. Discrepancies in the XAFS samples among various samples may be due to doping uniformity, as has already been noted.[6] Calculations characterizing the band structure with randomly distributed impurities will be documented in an upcoming article.

CONCLUSIONS

In summary, we performed DFT band structure calculations on the doped superconductor $La_{2-x}Sr_xCuO_4$ ($x=0.125$, 0.25, and 0.5) using the unrestricted spin form of the B3LYP functional. In a previous publication,[8] this functional was shown to provide a superior description of the undoped antiferromagnetic state of La_2CuO_4. Here, we showed it leads to a fundamentally different picture of the doped state as compared to the conventional LSDA description. Hole formation was found to be highly inhomogeneous, with localization adjacent to the Sr impurity. Most significantly, the symmetry of the hole was found to be z^2 as opposed to the commonly believed x^2-y^2. A triplet coupling between the A_{1g} doped holes and the B_{1g} intrinsic holes leads to the formation of a highly spin polarized z^2 band which lies in the middle of the insulating gap. We expect that a random distribution of Sr sites will profoundly affect the band structure, restoring the spin symmetry and approximate single unit cell symmetry, but producing significant lifetime effects. However, given the robustness of these results across a wide range of doping levels, we expect the basic nature of the doped hole should be largely unchanged from that presented here.

It is our firm view that the LSDA band structures from fourteen years ago have led the field astray. At this juncture, the *ab initio* evidence supports the formation of z^2 holes upon doping, and this must be taken into account in the analysis of normal state properties and in the development of models of superconductivity.

ACKNOWLEDGMENTS

We wish to acknowledge helpful discussions with Dr. Daniel Haskel and Dr. Peter Schultz. This work was partially supported by the Materials and Process Simulation Center (MSC) at Caltech which is supported by grants from DOE-ASCI, ARO/DURIP, ARO/MURI, 3M, Beckman Institute, Seiko-Epson, Dow, Avery-Dennison, Kellogg, and Asahi Chemical.

*URL: http://www.firstprinciples.com

[1] J. Yu, A.J. Freeman, and J.H. Xu, Phys. Rev. Lett. **58**, 1035 (1987); L.F. Mattheiss, *ibid.* **58**, 1028 (1987); W.E. Pickett, Rev. Mod. Phys. **61**, 433 (1989).

[2] A. Svane, Phys. Rev. Lett. **68**, 1900 (1992).

[3] W.M. Temmerman, Z. Szotek, and H. Winter, Phys. Rev. B **47**, 11 533 (1993).

[4] V.I. Anisimov, M.A. Korotin, J. Zaanen, and O.K. Andersen, Phys. Rev. Lett. **68**, 345 (1992).

[5] M.T. Czyzyk and G.A. Sawatsky, Phys. Rev. B **49**, 14 211 (1994).

[6] D. Haskel, E.A. Stern, D.G. Hinks, A.W. Mitchell, and J.D. Jorgensen, Phys. Rev. B **56**, R521 (1997); E.A. Stern, V.Z. Polinger, and D.A. Haskel, J. Synchrotron Radiat. **6**, 373 (1999); D. Haskel, E.A. Stern, F. Dogan, and A.R. Moodenbaugh, *ibid.* **8**, 186 (2001).

[7] J.K. Perry and J. Tahir-Kheli, Phys. Rev. B **58**, 12 323 (1998); J. Tahir-Kheli, *ibid.* **58**, 12 307 (1998); J.K. Perry, J. Phys. Chem. A **104**, 2438 (2000); J. Tahir-Kheli, *ibid.* **104**, 2432 (2000); J.K.

Perry and J. Tahir-Kheli, cond-mat/9907332 (unpublished); cond-mat/9908308, Phys. Rev B (to be published).
[8] J.K. Perry, J. Tahir-Kheli, and W.A. Goddard III, Phys. Rev. B **63**, 144510 (2001).
[9] A.D. Becke, J. Chem. Phys. **98**, 5648 (1993); C. Lee, W. Yang, and R.G. Parr, Phys. Rev. B **37**, 785 (1988).
[10] P.C. Hammel, B.W. Statt, R.L. Martin, F.C. Chou, D.C. Johnston, and S.-W. Cheong, Phys. Rev. B **57**, R712 (1998).
[11] V.R. Saunders, R. Dovesi, C. Roetti, M. Causà, N.M. Harrison, R. Orlando, and C.M. Zicovich-Wilson, *CRYSTAL98 User's Manual* (University of Torino Press, Torino, 1998).
[12] D.D. Johnson, Phys. Rev. B **38**, 12 807 (1988); C.G. Broyden, Math. Comput. **19**, 577 (1965).
[13] http://www.dl.ac.uk/TCS/Software/CRYSTAL
[14] P.J. Hay and W.R. Wadt, J. Chem. Phys. **82**, 299 (1985).
[15] R.M. Hazen, in *Physical Properties of High Temperature Superconductors II*, edited by D.M. Ginsberg (World Scientific, New Jersey, 1990), pp. 121–198.